ACS APPLIED POLYMER MATERIALS

pubs.acs.org/acsapm Article

# Transport Property Modulation via Solvent-Specific Behavior in Crosslinked Nonaqueous Membranes

Patrick M. McCormack, Gary M. Koenig, Jr.,* and Geoffrey M. Geise*

Cite This: ACS Appl. Polym. Mater. 2023, 5, 2449−2461 Read Online

ACCESS | Metrics & More | Article Recommendations | Supporting Information



**ABSTRACT:** Nonaqueous redox flow batteries (RFBs) are one economically promising solution for meeting grid-scale energy storage needs at discharge durations of 10 h or more. However, membrane transport properties in nonaqueous systems are not as well understood as in water. Solvent-specific effects complicate efforts to understand transport in nonaqueous systems. Changing the solvent used to measure membrane transport properties causes changes in solvent uptake, which can mask other solvent-specific differences and trends. This study decoupled these effects by using crosslinked membranes with post-crosslinking solvent exchange steps to vary the membrane solvent uptake of three solvents that are suitable for RFBs. This approach enabled the independent study of solvent uptake and specific measurement solvent effects on membrane transport properties. The results revealed differences in polymer solvation between the measurement solvents, and these differences led to changes in the sensitivity of both ionic conductivity and uncharged active material permeability to solvent uptake. Additionally, these changes in sensitivity appeared to be independent of each other, e.g., a weak dependence of ionic conductivity on solvent uptake coupled with a strong dependence of permeability on solvent uptake was observed for some materials. As a result, the highest-performing membrane, a crosslinked phenoxyaniline trisulfonate-functionalized poly(phenylene oxide) membrane produced using acetonitrile as the de-swelling solvent and characterized using propylene carbonate, retained a high conductivity of 0.20 mS $cm^{-1}$ while restricting active material permeability to less than $10^{-11}$ $cm^2$ $s^{-1}$. The reported solvent-specific behavior suggests that specific solvent−polymer interactions may provide a route to simultaneously increase ionic conductivity and decrease active material permeability, which would lead to more selective membranes to enable high-efficiency nonaqueous RFBs.

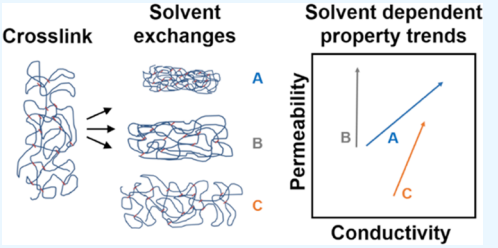


**KEYWORDS:** *nonaqueous selective membrane, lithium-ion-conducting membrane, separator, functional polymer, flow battery, energy storage*

## INTRODUCTION

The growing use of renewable, but nondispatchable, power sources like wind and solar has created a need for grid-scale energy storage with long discharge times (e.g., 10+ h) that currently are not common in grid-connected batteries.[1−3] Redox flow batteries (RFBs) have been proposed as an option for grid-scale energy storage, but one limitation for current aqueous electrolyte-based RFBs is relatively low volumetric energy density, which results from the electrochemical stability window of water and active material solubility.[4−6] Electrolytes prepared using organic solvents have a wider electrochemical stability window than aqueous electrolytes, and the chemistry of many organic redox active materials can be modified to enable very high solubility in organic solvents and higher energy density.[7−14] While many parts of the RFB have an impact on the overall efficiency and power density of the battery, the separators in nonaqueous RFBs are a limiting factor because of the lack of purpose-engineered materials for this application.[15] The separator must offer high ionic conductivity to provide high power density and voltage efficiency, and it must have low permeability of the dissolved active materials to prevent crossover that compromises battery longevity and/or coulombic efficiency.[7,16]

Different categories of separators have been proposed to meet these requirements, including micro- or nanoporous separators and ceramics, but this work focuses on dense polymer ion exchange membranes (IEMs).[7,15] These IEMs rely on connected pathways of charged regions to provide ionic conductivity, and they can restrict small-molecule transport based on kinetic (e.g., size) or thermodynamic (e.g., charge exclusion and/or secondary interactions) factors.[17]

The properties of IEM separators used with aqueous electrolytes have been extensively studied,[16−18] but solvent-specific effects that are unique to nonaqueous systems are not yet fully understood. Changes in solvent can profoundly impact the solvent uptake of the polymer. For example, many

Received: December 8, 2022
Accepted: March 17, 2023
Published: March 30, 2023

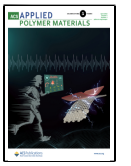

Scheme 1. Crosslinking of Br-PPO Using ODA

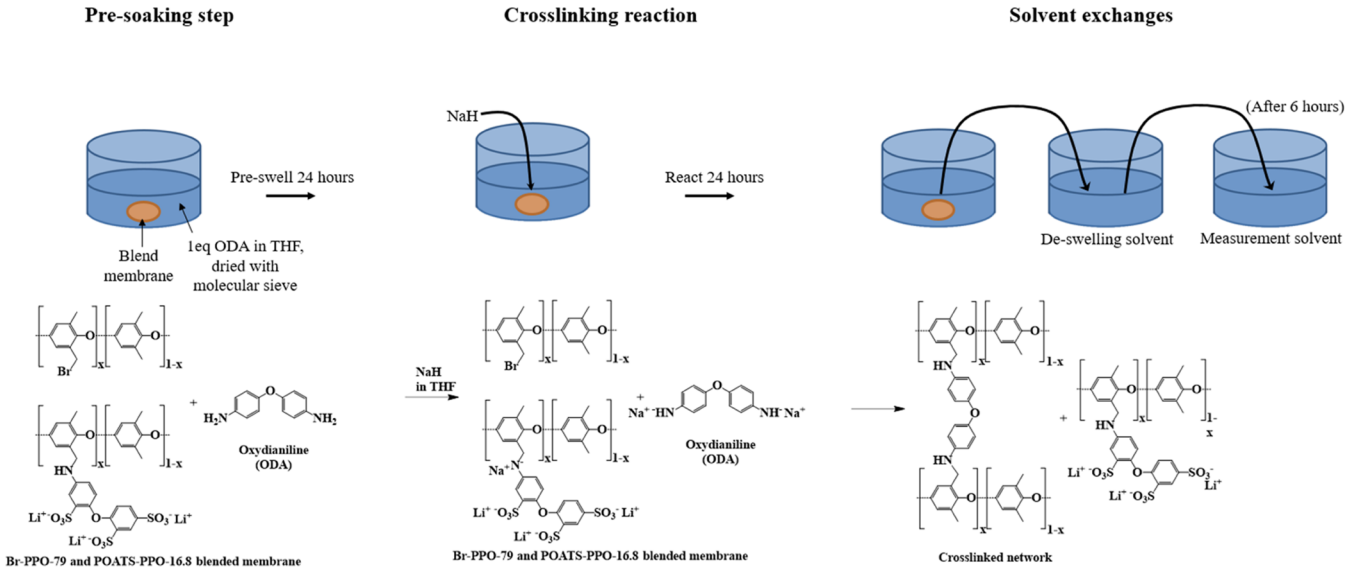


membranes, which are dimensionally stable in water, may swell excessively or dissolve upon exposure to organic solvents.[19] Even membranes that do not swell excessively can be subject to solvent-specific effects, which can lead to conductivity values much lower than expected based on solvent uptake and pure solution conductivity properties.[20]

Despite these differences, many nonaqueous RFB studies have used commercially available IEMs that were designed for use with aqueous systems.[7,19−22] Conductivity of these membranes has been reported to be highly dependent on the solvent and salt used to prepare the electrolyte, with conductivity for a single membrane varying from 0.001 to 10 mS $cm^{-1}$ in response to changing electrolyte conditions.[15,19] Conductivity differences were attributed largely to differences in solvent uptake because the highest conductivities often occurred when solvent uptake was 100% or more. High solvent uptake, however, has coincided with high active molecule permeability, of order $10^{-7}$ $cm^2$ $s^{-1}$.[20] Alternatively, membranes have been prepared to achieve permeability values as low as $10^{-10}$ $cm^2$ $s^{-1}$, but these low permeability values have accompanied low conductivity[15,23] in a manner consistent with general trade-off relationships between measures of membrane selectivity and throughput.[24−27]

A few IEMs have been developed specifically for nonaqueous RFB applications.[28−31] Increasing the fixed charge density (or the concentration of ionic charge carriers in the membrane) is a route for increasing ionic conductivity, but this approach also has led to increased swelling and therefore to high permeability.[23,28] To control swelling, some of these IEMs have been crosslinked to reduce the ability of the polymer to swell in solvents.[28,30−33] The swelling control afforded by crosslinking can keep permeability values low while allowing access to higher fixed charge concentrations that promote ionic conduction.[31]

For both commercial and novel membranes, solvent uptake has been shown to be a strong predictor of transport properties. However, in many prior studies, solvent uptake was not varied independently of polymer chemistry. The specific solvent used and the IEC of the polymer may influence transport properties independently, so it is important to decouple the relative impact of these factors on solvent uptake.

Our previously reported membranes, which are among the first CEMs to be targeted toward nonaqueous RFBs, relied on a high glass-transition temperature backbone polymer to achieve the swelling resistance necessary to maintain polymer dimensional stability in a range of organic solvents.[15,23] Herein, sulfonated poly(phenylene oxide) (PPO) polymers, similar to those in our prior work,[23,34] were crosslinked via a strategy that introduced crosslinks into the noncharged regions of the membrane, followed by a series of solvent exchange steps to produce membranes with different solvent uptake from the same starting material. This strategy was intended to control organic solvent swelling in the noncharged regions of the polymer, as opposed to other approaches that crosslink the charged regions of the polymer.[28,30,31]

Our crosslinking procedure yielded different final membranes, prepared from a single starting polymer, with a range of solvent uptake properties. This approach isolated the effects of solvent uptake on membrane properties from other experimental variables, e.g., membrane IEC or the measurement solvent. Additionally, the approach enabled the preparation of mechanically robust membranes with higher total fixed charge density (to facilitate ionic conduction) relative to our previous study that was limited by mechanical properties in the absence of crosslinking.[23] This library of membranes with different solvent uptake properties characterized using multiple measurement solvents enabled the study of ionic conductivity and uncharged small-molecule transport through the membranes. Particularly for nonaqueous RFB applications, it is critical to understand relevant trade-offs in transport properties to guide the design of system components including membrane, electrolyte/solvent, and active material to meet nonaqueous RFB requirements.

## METHODS

**Overall Membrane Preparation Strategy.** Crosslinked membranes were formed by blending brominated poly(phenylene oxide) (Br-PPO) with the ion exchange polymer, phenoxyaniline trisulfonate-substituted PPO (POATS-PPO), prior to film casting. Then, a bifunctional molecule (oxydianiline, ODA), which reacts with Br-PPO, was added to crosslink the blend membrane without forming a fixed charge group (Scheme 1). Photographs of the cast crosslinked



https://doi.org/10.1021/acsapm.2c02121
ACS Appl. Polym. Mater. 2023, 5, 2449−2461

membranes at different stages of the crosslinking process are shown in the Supporting Information (Figure S1).

Crosslinking was performed while the cast membranes were swollen in tetrahydrofuran, THF, (~150% uptake by mass). Swelling in THF was necessary to allow ODA to diffuse into the membrane and to permit the subsequent reaction between ODA and the bromine functional group on Br-PPO. Following the crosslinking reaction between ODA and Br-PPO, the membranes were not allowed to dry. Rather, the THF was removed by exchanging it with a different solvent, called the de-swelling solvent. In this study, the de-swelling solvent was either water, ethanol, or acetonitrile (ACN).

The solvent exchange process following crosslinking was designed to take advantage of effects similar to membrane casting by phase inversion with a nonsolvent. In the phase inversion casting process, a support coated with polymer dissolved in solution is immersed quickly in a nonsolvent for the polymer, and mixing of the solvent and nonsolvent causes the polymer to come out of solution and solidify rapidly.[35] The specific nonsolvent used can affect the final membrane morphology by changing how quickly the precipitation and solvent exchange steps occur,[36] and we hypothesized that similar morphological or structural differences could be achieved by swelling our polymer to a large extent (i.e., ~150% using THF), then quickly replacing the strongly swelling THF with one of the less strongly swelling de-swelling solvents.

The de-swelling process led to tunable property differences in the membranes that persisted even after the de-swelling solvent was replaced yet again with a measurement solvent, which was selected from a range of suitable solvents used in nonaqueous flow batteries: dimethyl carbonate (DMC), propylene carbonate (PC), or ACN. Measured membrane physical and electrochemical properties depended on both the de-swelling solvent history and the measurement solvent used for characterization. Membranes were referred to by the solvents used in these two exchanges. For example, a membrane that was prepared using ethanol as the de-swelling solvent and characterized using DMC as the measurement solvent was be referred to as an ethanol/DMC membrane.

**Br-PPO Synthesis.** Br-PPO was synthesized via a free radical bromination reaction of poly(phenylene oxide), PPO (Sigma-Aldrich).[23] The amounts of the bromine source (*N*-bromosuccinimide, NBS, >98%, TCI Chemicals) and free radical initiator (azobisisobutyronitrile, AIBN, 98%, Sigma-Aldrich), relative to PPO, were varied to obtain different degrees of bromination. In this work, Br-PPO with bromine substitution of 16.6% at the benzyl position of PPO repeat units was used for producing POATS-PPO, and Br-PPO with a bromine substitution of 79% was used for crosslinking, measured by $^1$H NMR (Supporting Information, Figure S3); these materials were referred to as Br-PPO-16.6 and Br-PPO-79.[23] Preparation of both materials began by dissolving 6 g of PPO in 75 mL of chlorobenzene and heating in a 110 °C oil bath. For Br-PPO-16.6, a total of 3.2 g of NBS and 0.179 g of AIBN were pre-weighed, evenly distributed into 4 glass vials, and stirred to mix the powders. This amount of NBS could theoretically result in Br-PPO-36, so the yield of this substitution was approximately 46%. For the Br-PPO-79, a total of 10.0 g of NBS and 0.561 g of AIBN were used, and divided into 4 glass vials in the same way. This amount of NBS could theoretically result in Br-PPO-112, so the yield of this substitution was approximately 71%. Each vial of mixed NBS and AIBN powder was then added to the reaction flask containing the PPO solution, at intervals of 15 min between each addition. Sequential addition of NBS and AIBN over the course of 45 min, when preparing highly brominated Br-PPO, limited $Br_2$ formation and reduced undesired bromination at the aromatic positions.[37,38] The reaction proceeded at 110 °C for 30 min after the last NBS and AIBN addition (total reaction time of 75 min), and the product was collected by precipitating the reaction mixture in 10-fold excess reagent alcohol. The polymer was collected by filtration and dried under vacuum to remove the alcohol. A second purification was performed by dissolving the polymer in 50 mL of chloroform and repeating the precipitation in reagent alcohol followed by filtration and drying.

**Phenoxyaniline Trisulfonate (POATS) Synthesis.** POATS was synthesized using an aromatic sulfonation of 4-phenoxyaniline, reported previously.[23] Briefly, 2 g of 4-phenoxyaniline was dissolved in 15 mL of 20% fuming sulfuric acid, under stirring in an ice bath. Then, over the course of 30 min, the reaction temperature was raised to 80 °C and held at that temperature for 2 h. To end the reaction, the mixture was poured slowly over ice made from deionized (DI, 18.2 MΩ cm, Direct-Q 3 UV, Millipore) water and then was diluted, with DI water, to a total volume of 500 mL. Triethylamine (TEA) was added in an equimolar amount with regard to the theoretical number of aromatic sulfonate groups (4.5 mL of TEA in this example). Then, calcium carbonate was added to neutralize the remaining sulfuric acid (typically ~30 g). The precipitated calcium sulfate was filtered out, and the collected liquid solution was dried in a rotary evaporator at 70 °C. The remainder of the calcium sulfate was removed by dissolving the $TEA^+$ counter-ion form POATS in 15 mL of DI water and filtering out the undissolved solids. The POATS solution was then dried first in an oven at 80 °C for 16 h and then under vacuum at room temperature for an additional 24 h. The yield of $TEA^+$ counter-ion form POATS was approximately 76%.

**POATS-PPO Synthesis.** POATS-PPO was produced using an updated procedure, relative to previous reports,[23,34] which resulted in better yields at higher degrees of substitution. To limit water contamination, all reactants and glassware were dried under room-temperature vacuum for 24 h prior to reaction, and all solvents were stored over 3 Å molecular sieve for a minimum of 48 h before use. In an example procedure, 0.6 g of Br-PPO-16.6 was dissolved in a mixture of 4 mL of NMP and 4 mL of chlorobenzene, and 1.09 g of POATS (2 equiv, relative to the moles of Br) was dissolved separately in 16 mL of NMP. The two solutions were added to a stirred reaction flask that contained 250 mg $NaHCO_3$. The mixture was heated in a 60 °C oil bath for 24 h and then precipitated in 300 mL of isopropyl alcohol. The suspension was centrifuged, and the liquid was decanted. The solid product was washed first with an aqueous solution containing 0.1 M HCl and 0.11 M TEA, to ensure the amine groups in the product were deprotonated and the sulfonate groups were in the TEA counter-ion form, and then washed with DI water to remove free salt. The solid product was isolated after each washing step via centrifugation and decantation. Finally, the POATS-PPO product was dried under vacuum for 24 h before further use.

**Crosslinked Membrane Synthesis.** Reactive bromine groups were required for the crosslinking reaction. The POATS substitution of Br-PPO to form POATS-PPO, however, proceeded to completion. To provide bromine groups for the crosslinking procedure, POATS-PPO-16.6 and Br-PPO-79 solutions were mixed together and cast to form a blend membrane.

To prepare a typical membrane, 0.167 g of POATS-PPO-16.6 and 0.033 g of Br-PPO-79 were dissolved together in 2 mL of DMF. This degree of bromination and polymer mass ratio leads to a theoretical maximum crosslink density of 0.43 mmol crosslinks $g^{-1}$. The blend membrane was cast by pouring this solution into 6 cm diameter PTFE molds, and the polymer was dried first in an 80 °C convection oven for 4 h and subsequently in an 80 °C vacuum oven for 24 h. After drying, the sulfonate groups in the blend membranes were converted to the $Li^+$ counter-ion form by soaking the films in a 0.5 M lithium chloride solution for 8 h. The solution was replaced with fresh solution following the first 4 h of soaking. Finally, the film was soaked in DI water for 2 h and then dried under vacuum at room temperature for 24 h. A typical final membrane prepared via this route was approximately 60 $\mu$m thick and had a mass of 0.16 g, due to mass losses from transferring and casting the viscous polymer solution and from conversion from the $TEA^+$ (102 g $mol^{-1}$) counter-ion form to the much lighter $Li^+$ (7 g $mol^{-1}$) counter-ion form.

Bromine sites on the Br-PPO in the blend membrane were used to crosslink the material using ODA as the crosslinker. The procedure began by pre-swelling and removing trace water from the blend membrane by soaking the film in a solution of 1 mg $mL^{-1}$ ODA in THF that was mixed with 2 g of 4 Å molecular sieve powder in a glass jar that allowed the membrane to lay flat for 24 h. The volume used in this initial procedure was chosen to achieve an equimolar match of the



https://doi.org/10.1021/acsapm.2c02121
ACS Appl. Polym. Mater. 2023, 5, 2449−2461

**Table 1. Electrolyte Solvent Properties**

| solvent | viscosity (cP) | dielectric constant | density (g mL$^{-1}$) | conductivity of 1 M LiFSI (mS cm$^{-1}$)[a] | ferrocene solution diffusivity (cm$^2$ s$^{-1}$)[b] | 4-hydroxy-TEMPO solution diffusivity (cm$^2$ s$^{-1}$)[b] |
|---|---|---|---|---|---|---|
| propylene carbonate | 2.52[42] | 64.9[42] | 1.20[42] | 6.7 | $4.93 \times 10^{-6}$ | $4.46 \times 10^{-6}$ |
| dimethyl carbonate | 0.59[42] | 3.1[42] | 1.06[42] | 6.9 | $2.00 \times 10^{-5}$ | $1.80 \times 10^{-5}$ |
| acetonitrile | 0.34[41] | 35.9[43] | 0.79[41] | 37 | $2.33 \times 10^{-5}$ | $2.11 \times 10^{-5}$ |

[a]Measured with conductivity probe at room temperature, 20 °C. [b]Calculated using the Wilke−Chang correlation (details in the Supporting Information).

ODA amine groups and the Br groups present in the blend membrane, e.g., 13.8 mL of ODA in THF solution for a 0.16 g blend membrane.

The crosslinking reaction was initiated by adding 0.1 g of 60% NaH in mineral oil to the soaking solution, and the mixture was allowed to react for 24 h at room temperature. The reaction was quenched by removing the membrane from the solution and quickly transferring it to a de-swelling solvent: water, ethanol, or ACN. The membranes were soaked in the de-swelling solvent for 6 h to remove THF from the membrane.

Finally, the membranes were moved to the measurement solvent: DMC, PC, or ACN. This solvent was replaced once after 24 h to minimize the amount of de-swelling solvent present in the final membrane. The final membrane thickness, while swollen in measurement solvent, increased slightly relative to the non-crosslinked membranes, where membranes de-swelled in water and measured in PC had the highest average final thickness (75 $\mu$m). Membrane samples were stored in the measurement solvent until use, and this use of three de-swelling solvents and three measurement solvents resulted in a matrix of nine membrane processing conditions that were subsequently characterized.

**Membrane Solvent Uptake and Solvent Volume Fraction.** Solvent uptake was measured by removing the crosslinked membranes from the measurement solvent, quickly wiping the surface to remove excess liquid, and weighing the membrane to determine the solvated mass. Membrane pieces were then dried for 24 h at room temperature under vacuum (for DMC and ACN measurement solvents) or 72 h at 80 °C under vacuum (for PC measurement solvent), and the sample dry (i.e., effectively solvent-free) mass was determined. To ensure the membranes were fully dried (i.e., solvent was effectively removed), samples were returned to the vacuum chamber for an additional 24 h after which their mass was unchanged. Solvent uptake, SU, was calculated as

$$\mathrm{SU} = 100\% \times \frac{\text{solvated mass} - \text{dry mass}}{\text{dry mass}} \tag{1}$$

Solvent uptake was converted to solvent volume fraction, $\Phi$, using dry membrane and solvent densities and by assuming volume additivity

$$\Phi = \frac{\mathrm{SU}}{\mathrm{SU} - \frac{\rho_{\text{solvent}}}{\rho_{\text{poylmer}}}} \tag{2}$$

where $\rho_{\text{solvent}}$ is the density of the measurement solvent (Table 1) and $\rho_{\text{poylmer}}$ was taken as the density of the dry non-crosslinked blend membrane. It was assumed that the density of the polymer did not change appreciably after crosslinking (since ODA was chemically very similar to the chemistry of the rest of the polymer), and the dry density was measured to be 1.38 g mL$^{-1}$ via the procedure described subsequently.

Polymer dry density was measured using an Archimedes' principle method.[39] The mass of the dry non-crosslinked blend membrane was measured in air while the membrane was submerged in cyclohexane. The blend membrane sorbed a negligible amount of cyclohexane over the timescale of the experiment. With the membrane masses measured in air and cyclohexane ($m_{\text{air}}$ and $m_{\text{cyclohexane}}$, respectively) and the known densities of air and cyclohexane ($\rho_{\text{air}}$ and $\rho_{\text{cyclohexane}}$, respectively) at the measurement temperature, dry membrane density, $\rho_{\text{polymer}}$, was calculated as

$$\rho_{\text{polymer}} = \frac{m_{\text{air}}}{m_{\text{air}} - m_{\text{cyclohexane}}}(\rho_{\text{cyclohexane}} - \rho_{\text{air}}) - \rho_{\text{air}} \tag{3}$$

**Ion Exchange Capacity (IEC).** The fixed charge density of the polymer was quantified as the IEC, which was reported as milliequivalents of sulfonate groups per gram of dry (i.e., effectively solvent-free) polymer (mequiv g$^{-1}$). To measure the IEC of the membrane via a titration method, samples were soaked in 0.5 M HCl for 24 h at room temperature to convert the fixed charge groups from the $Li^+$ counter-ion form to the acid ($H^+$) counter-ion form. Samples were then moved to DI water, which was replaced three times and allowed to soak for 1 h each time.

The secondary amines formed during the addition of POATS and ODA molecules to the Br-PPO can act as a base during the acid-soaking process. Therefore, this initial step of the IEC measurement process may have resulted in more uptake of acidic protons than is required to replace completely the $Li^+$ counter-ions with $H^+$ counter-ions because of acid-base chemistry that can occur with the secondary amines that connect the crosslinker and side chain to the polymer backbone. Additional acid uptake via this process would interfere with the IEC measurement. To ensure that the secondary amines in the polymer were deprotonated, the pH of the last DI water-soaking solution was measured and verified to be above pH 6.

Following the DI water-soaking step, the membranes were moved to a 0.1 M $CaCl_2$ solution for 24 h at room temperature to convert the sulfonate groups to the calcium counter-ion form and release the protons into solution. This solution was then titrated with 0.01 M NaOH to measure the amount of $H^+$ released by the membrane during the ion exchange process to the calcium counter-ion form. The final pH of this solution (after soaking) was typically around 3, so some of the acid released from the sulfonate groups could have been absorbed by protonation of the secondary amine groups in the membrane and thus not be accounted for during the titration. To account for this retained acid, the membrane was left to soak in the neutralized solution (following the first titration) for 24 h. Subsequently, the solution was titrated a second time to measure the additional acid released from the secondary amines in the material. The membranes were then dried in an 80 °C vacuum oven for 24 h, and the dry mass was measured. The IEC was calculated as

$$\text{IEC [mequiv g}^{-1}] = \frac{V_{0.01\text{M NaOH}} \times 10\ \text{mM}}{m_{\text{dry}}} \tag{4}$$

where the total volume of titration solution (from both titrations), $V_{0.01\text{M NaOH}}$ (L), and the membrane dry mass, $m_{\text{dry}}$ (g).

**Ionic Conductivity.** Ionic conductivity was measured using through-plane electrochemical impedance spectroscopy (EIS).[22] Membranes soaked in DMC, PC, or ACN measurement solvents were cut into 0.75-inch diameter circles and moved to a 1.0 M LiFSI solution made using the same measurement solvent (either DMC, PC, or ACN solvent, respectively). Membranes were placed in a BioLogic controlled environment sample holder (CESH), with 0.5-inch diameter circular electrodes. Impedance was measured using a potentiostat (BioLogic SP-300) to impose an oscillating potential with a 20 mV amplitude over a frequency range of 1 MHz to 100 Hz, an example spectrum can be found in Supporting Information, Figure


https://doi.org/10.1021/acsapm.2c02121
ACS Appl. Polym. Mater. 2023, 5, 2449−2461

S4. The resulting data were fit to a model circuit, and the high-frequency intercept with the real impedance axis was used to determine the membrane resistance.[22] This intercept resistance also included the cell resistance, and the cell resistance was measured (with no membrane present in the cell) and subtracted from the value obtained when the membrane was loaded in the cell to determine the membrane resistance, $R$ (in Ω). Cell resistance was low compared to membrane resistance values (typically 0.5 Ω for the cell compared to 10−50 Ω for the membranes). Following the EIS measurement, membranes were removed from the sample holder, and sample thickness was measured in three places and averaged. Resistance was converted to ionic conductivity, $\sigma$, as

$$\sigma\ [\mathrm{mS\ cm^{-1}}] = 1000\left(\frac{l}{RA}\right) \tag{5}$$

where $l$ is the average sample thickness in cm and $A$ is the area of the electrodes, 1.27 $cm^2$. Membranes evaluated were always larger than the electrode area.

**Permeability.** Permeability was measured using a glass H-cell.[20,23] The cell was assembled with a membrane (pre-soaked in DMC, PC, or ACN measurement solvent) separating the two halves of the cell. One half of the cell contained 0.1 M active material (either ferrocene or 4-hydroxy-TEMPO) in the same measurement solvent used to pre-soak the membrane, and the other half of the cell (i.e., the blank side) initially contained pure measurement solvent. The active material concentration of the solution in the blank side of the cell, which increased as active material permeated through the membrane, was measured three times using UV−vis spectroscopy.

The measurement frequency was chosen based on the rate of crossover so that all three measurements would be within the calibration range of the UV−vis measurement technique and roughly evenly spaced in time. Calibration curves and concentration ranges for ferrocene and 4-hydroxy-TEMPO can be found in the Supporting Information, Figure S5. In this report, the highest permeability values were measured using a 2 h measurement interval, and the lowest permeability values were measured with a 10-day measurement interval. After the last measurement, the cell was disassembled, and the thickness of the sample was measured. The permeability was calculated as

$$Pt = -\frac{V_L l}{2A}\ln\left(1 - 2\frac{C_R[t]}{C_D[0]}\right) \tag{6}$$

where $P$ is permeability in $cm^2\ s^{-1}$, $V_L$ is the volume on each side of the membrane in mL, $l$ is the membrane thickness in cm, $A$ is the cross-sectional area of the membrane exposed to solution in $cm^2$, $C_R[t]$ is the measured active material concentration of the solution in the blank side of the cell at time $t$, and $C_D[0]$ is the initial active material concentration (0.1 M) of the solution on the other side of the membrane.

## RESULTS AND DISCUSSION

**Measurement Solvent Uptake.** A series of crosslinked membranes with varied solvent uptakes were produced via two solvent exchange steps. First, a de-swelling solvent exchange step removed the highly swelling THF reaction solvent. Next, the de-swelling solvent was replaced, via a second exchange, with the measurement solvent that was used for transport property evaluation: PC, DMC, or ACN. The measurement solvents were chosen because they can be used as electrolyte solvents in RFBs. Cyclic and linear carbonates, including PC and DMC, have been studied extensively as lithium-ion battery electrolytes, and ACN is popular as a nonaqueous RFB electrolyte due to its high ionic conductivity and low viscosity.[40,41] These measurement solvents also have different physical properties, e.g., viscosity and dielectric constant, which could affect how they solvate the membranes. The relevant physical and electrochemical properties of the solvents, electrolytes, and active material solutions are shown in Table 1.

The differences in solvent uptake created by the de-swelling solvent persisted after the de-swelling solvent was replaced by the measurement solvent (Figure 1a). In general, the ethanol

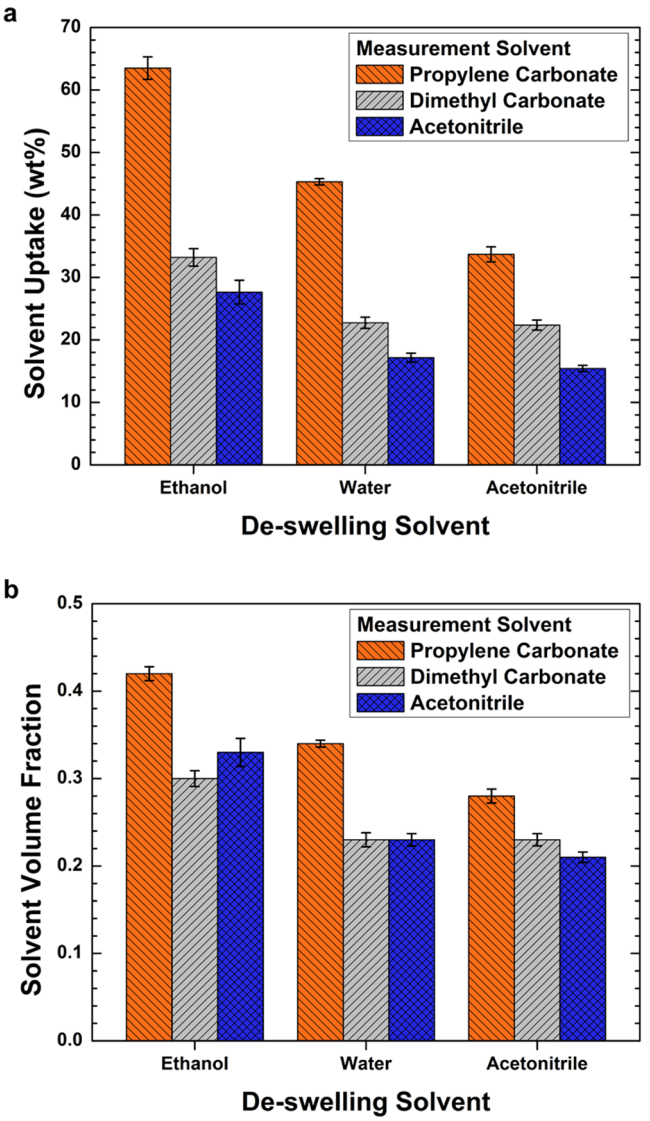


**Figure 1.** Measurement solvent uptake, expressed as the (a) mass of measurement solvent sorbed as a percentage of the dry polymer mass and (b) measurement solvent volume fraction in the swollen polymer. Measurement solvent uptakes of propylene carbonate (orange), dimethyl carbonate (gray), and acetonitrile (blue) are reported as a function of the de-swelling solvent used in the crosslinking procedure. The reported values are the average of values measured using three different membrane samples, and the reported uncertainty is the standard deviation of the average of each set of three membranes.

de-swelling solvent resulted in the highest uptake values followed by water and ACN, which tended to have similar uptakes by comparison. This trend was the same as the solvent uptake trend of the three de-swelling solvents in non-crosslinked membranes (in the absence of solvent exchange steps) with solvent weight uptakes of 50, 26, and 20% for ethanol, water, and ACN, respectively. Within each specific de-swelling solvent, the measurement solvent PC led to the highest uptake, whereas ACN (in its role as a measurement


https://doi.org/10.1021/acsapm.2c02121
ACS Appl. Polym. Mater. 2023, 5, 2449−2461

solvent) resulted in the lowest uptake. Notably, the solvent weight uptake of ACN de-swelled membranes, with ACN as the measurement solvent, had a lower solvent weight uptake than the non-crosslinked membrane ACN uptake (15 vs 20%). This result suggested that either the crosslinking procedure lowered equilibrium uptake, or the solvent exchange process caused the polymer morphology to change to a lower solvent uptake configuration.

The solvent exchange process from THF to the de-swelling solvent resulted in visible differences in the membrane that were de-swelling solvent-specific (photographs in Figure S1). Solvent exchange from THF to ACN shrank the membrane to approximately its original size before the THF swelling process. Exchange from THF to either water or ethanol had much less of an influence on membrane swelling, and the resulting membranes had a larger diameter than both the ACN de-swelled membrane and the membrane diameter before exposure to THF.

Solvent volume fraction was also considered because the measurement solvents had different densities and transport properties often correlate strongly with solvent volume fraction, as opposed to mass fraction.[44] Solvent volume fraction generally mirrored the qualitative solvent uptake results (Figure 1b) and to some extent attenuated differences between the de-swelling and measurement solvent effects.

The sensitivity of uptake and swelling results to solvent history may be a result of the glassy nature of the PPO backbone. The de-swelling solvent may establish a chain configuration that was then locked into place by the kinetically trapped nature of the glassy polymer chains. Similar solvent-based effects have been leveraged in commercial membrane applications, though many of these details are often regarded as industrial art.[45]

Both the de-swelling and measurement solvents affected the final solvent volume fraction of the membrane, and the de-swelling solvent most significantly influenced the volume fraction of PC in the membrane. Membrane swelling was not as strongly influenced by the use of either DMC or ACN as the measurement solvent, but the use of ethanol as the de-swelling solvent did lead to higher measurement solvent uptakes compared to the other two de-swelling solvents.

The higher measured solvent volume fraction of PC compared to DMC and ACN may be due to differences in how the charged regions of the polymer interact with the measurement solvent. PC had a higher dielectric constant than either DMC or ACN (Table 1), which may have led to stronger solvation of the charged sulfonate groups of POATS. Although the $Li^+$ counter-ion form of POATS was not significantly soluble in any of these solvents, the $TEA^+$ counter-ion form of POATS was soluble in PC, while it was not soluble in ACN or DMC. This observation further suggested a greater affinity between POATS and PC compared to POATS and either DMC or ACN, which could have resulted in the observed higher solvent uptakes.

The crosslinking and solvent exchange procedures represent changes to POATS-PPO processing relative to previous reports.[23,34] To provide evidence of the critical role of the crosslinking step, materials were also prepared without adding NaH to investigate the effects of the solvent exchange process without crosslinking the membranes. However, the non-crosslinked membranes could not withstand the stress created by the de-swelling process, and they did not remain intact (Figure S2). Membrane IECs were also measured before and after crosslinking, and the IEC was unchanged by the procedure (2.5 mequiv $g^{-1}$) suggesting no charge group degradation. These control experiments, and consideration of other possible side reactions, are discussed in more detail in Supporting Information Section S6.

**Ionic Conductivity.** Membrane ionic conductivity was measured using 1.0 M LiFSI electrolytes in each of the measurement solvents (Figure 2a) because of the high solution conductivity and good stability of LiFSI,[40] and the measured area specific resistance values are also reported in Figure S6. The POATS-PPO material contained a high concentration of $Li^+$ charge carriers, with an IEC of 2.5 mequiv $g^{-1}$, and such materials often have high cation transference numbers.[7] As such, ionic conduction in POATS-PPO was assumed to result primarily from migration of $Li^+$. The ionic conductivity of membranes soaked in electrolytes prepared using both

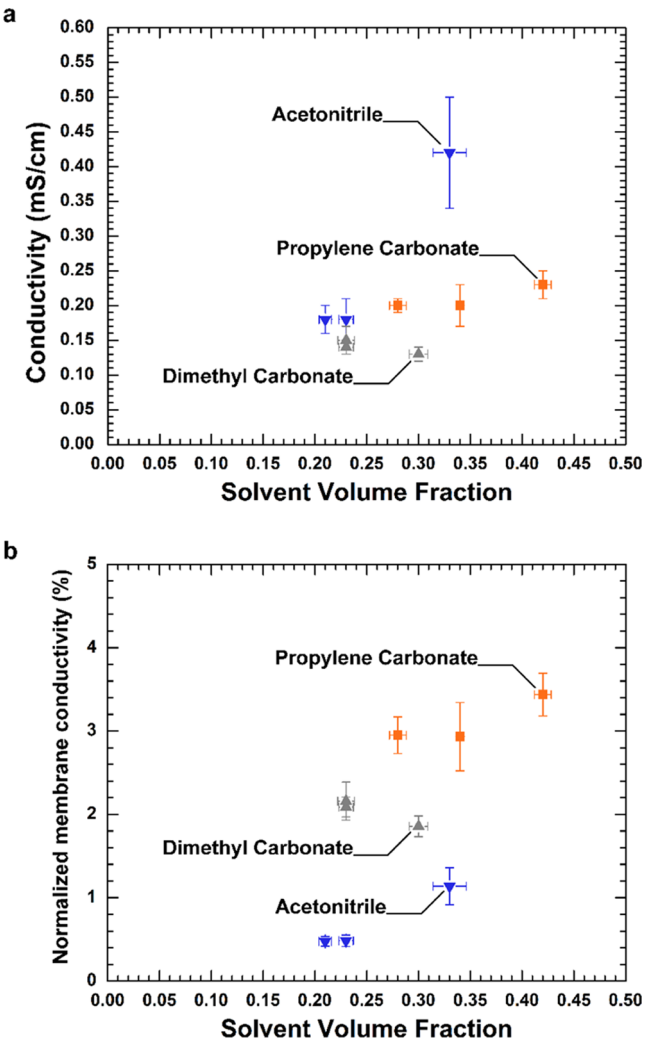


**Figure 2.** (a) Membrane conductivity and (b) membrane conductivity as a percentage of the bulk electrolyte solution conductivity as a function of measurement solvent volume fraction. The membrane conductivity values were measured using crosslinked membranes immersed in 1.0 M LiFSI in either propylene carbonate (orange), dimethyl carbonate (gray), or acetonitrile (blue). All reported values of membrane conductivity and solvent volume fraction are the average of the values measured using three different membrane samples, and the reported uncertainty is the standard deviation of average for each membrane set.


https://doi.org/10.1021/acsapm.2c02121
ACS Appl. Polym. Mater. 2023, 5, 2449−2461

carbonate solvents was relatively independent of solvent volume fraction, with the DMC values specifically not having a statistically significant difference. Membranes measured in ACN had a more significant dependence on solvent volume fraction, where the ethanol/ACN membranes specifically had a higher membrane conductivity than the other membranes measured using the ACN electrolyte. The solution conductivity of the ACN electrolyte was higher than that of either carbonate electrolyte (Table 1), so the membrane conductivity may have been more sensitive to ACN electrolyte uptake.

Direct correlation between solvent uptake and conductivity has previously been observed, but solvent uptake typically changes as a result of another change to the system, such as the membrane IEC or electrolyte composition.[19,20,31] In the present study, changes in solvent uptake were imposed by the use of different de-swelling and measurement solvents. Previous POATS-PPO results showed an increase in conductivity from 0.015 to 0.061 mS $cm^{-1}$ as solvent uptake increased from 31 to 39%. This change likely was driven by an increase in IEC from 0.75 to 1.17 mequiv $g^{-1}$, and was a larger relative change in conductivity than was observed using any measurement solvent in Figure 2. Not all reports in the literature show as strong a dependence of conductivity on solvent uptake as these examples, even in systems where solvent uptake was increased by increasing the IEC. In one report, conductivity changed from 0.14 to 0.34 mS $cm^{-1}$ with a solvent uptake change from 12 to 26%,[28] and another report showed a conductivity change from just 0.08 to 0.11 mS $cm^{-1}$ with a thickness ratio change from 2 to 11%,[31] where both of these reports also had changes to IEC.

In our work and that of others, the dependence of conductivity on solvent uptake appeared to be solvent or polymer specific. In ACN, the conductivity more than doubled (comparing the lowest solvent volume fraction to the highest), but with PC and DMC, no statistically significant change was observed. Similar solvent-specific behavior has been observed in Nafion-like membranes, i.e., polymers with the same structure as Nafion, but different equivalent weights (i.e., IEC values).[46] Generally, Nafion conductivity increases with solvent uptake when the uptake changes as a result of changing the solvent, but data of this type in the literature has been reported with a large amount of scatter.[19] The solvent uptake alternatively can be varied by changing the equivalent weight of the material, and these changes had large impacts on conductivity for some solvents, but in other solvents, the changes in conductivity with changing solvent uptake were less pronounced.[46]

For example, comparing 1200 g $equiv^{-1}$ (IEC = 0.83 mequiv $g^{-1}$) and 800 g $equiv^{-1}$ (IEC = 1.25 mequiv $g^{-1}$) Nafion, the water uptake of these membranes increased from 25 to 380% uptake, respectively, and PC uptake also increased significantly from 30 to 175% uptake as the IEC increased.[46] Despite the increase in water uptake, the $Li^+$ conductivity of the two water-soaked membranes was nearly identical, but in the PC-soaked membranes, the $Li^+$ conductivity of the 0.83 mequiv $g^{-1}$ membrane was approximately 30 times lower than the 1.25 mequiv $g^{-1}$ membrane. In both cases, changes in equivalent weight (IEC) resulted in different uptake properties, but in water, those changes did not affect ionic conductivity, whereas they did in PC. The increased solvent uptake of the higher IEC membranes results in a lower charge density, due to increased membrane volume. This decrease in fixed charge density appears to have different impacts on the membrane conductivity depending on the measurement solvent, i.e., conductivity in PC is more affected than conductivity in water.

The fixed charge density of the crosslinked membranes reported can be found in Figure S7. These differences could be a result of differences in ion solvation by the different solvents. Studies of Li-ion battery electrolytes have shown that PC, DMC, and ACN have different ion solvation characteristics, i.e., the fraction of ions that exist as free ions, solvent-separated ion pairs, or contact ion pairs changed depending on solvent, salt, and concentration.[47−51] These differences in the ion pairing and solvation characteristics may lead to differences in sensitivity to charged group spacing. Thus, in our work, the solvent-specific relationship between conductivity and solvent uptake may be related to the physical fixed charge group spacing in the membranes and the specific mechanism of charge transport and solvation in each solvent.

Solvent-specific effects can be investigated further by considering the bulk electrolyte conductivity of the different measurement solvents (Table 1). The membrane ionic conductivity data were normalized by the conductivity of bulk 1.0 M LiFSI electrolyte in each of the measurement solvents (Figure 2b). Normalization in this manner attempted to account for differences in conductivity that were intrinsic to a specific solvent, and it emphasized the extent to which the polymer impeded the conduction process. Figure 2b shows that the polymer environment leads to dramatically reduced ionic conductivity (by at least 96%) relative to that of the bulk electrolyte for all of the measurement solvents considered.

The high ionic conductivity of POATS-PPO observed when using the ACN measurement solvent (Figure 2a) was speculated to result largely from the high ionic conductivity of 1.0 M LiFSI in ACN (as opposed to in PC or DMC) (Table 1). The data in Figure 2b, however, suggest that interactions between LiFSI, ACN, and the polymer act to restrict conduction in a manner that overcomes the highly conductive nature of LiFSI in ACN relative to the other two measurement solvents. Alternatively, specific polymer/measurement solvent interactions reduced conductivity to a lesser extent when PC was used as opposed to the other two measurement solvents. Ultimately, the data in Figure 2 suggest that the inherent conductivity of LiFSI in the measurement solvents was insufficient to explain the ionic conductivity of the membrane. Rather, solvent-specific effects appear to play an important role.

One solvent-specific property that could result in these observations is the dielectric constant since it is often related to the ability of a solvent to dissociate a salt, necessary for ionic conductivity.[19,52] Of the three measurement solvents, PC had the highest dielectric constant (Table 1), and the ratio of membrane conductivity to solution conductivity was greatest when PC was used (Figure 2b). However, DMC had the lowest dielectric constant but not the lowest ratio of membrane conductivity to solution conductivity. This behavior has also been noted in bulk electrolytes of $LiPF_6$ in mixtures of ethylene carbonate (EC) and DMC, where despite the difference in dielectric constant (90 vs 3.1), both EC and DMC participate in ion solvation.[49] An explanation for the ion solvation properties observed while using DMC (given its low dielectric constant compared to other common electrolyte solvents) is the change in conformation of the methyl groups of the DMC molecule.[51] Although the more stable cis-cis conformation of DMC has a low dielectric constant, MD simulations have suggested that coordination with $Li^+$ stabilizes the much more


https://doi.org/10.1021/acsapm.2c02121
ACS Appl. Polym. Mater. 2023, 5, 2449−2461

polar cis-trans conformer, which causes an increase in the dipole moment from 0.34 to 3.76.[49] This stabilization and resulting change in the dipole moment likely increases the DMC dielectric constant in the environment near ions relative to bulk property measurements.[51] As a result, the ability of DMC to solvate ions in the membrane may be higher than the dielectric constant suggested in Table 1, and this difference could help to promote $Li^+$ conduction in the membrane when DMC is used as the measurement solvent.

Even with high dielectric constant solvents like PC, dissociation of fixed charge groups in the polymer may be low. The $Li^+$ counter-ion form of POATS was not particularly soluble (<1 mg $mL^{-1}$) in DMC, PC, or ACN, and this observation suggested that dissociation of the POATS sulfonate groups was not favorable in these solvents. Other work has demonstrated that polymer charge groups which more easily dissociate in nonaqueous solvents, i.e., triflurormethanesulfonylimide, led to higher membrane ionic conductivity than an equivalent membrane with sulfonate groups.[53,54]

This observation was also consistent with Nafion data; reported conductivities in PC, DMC, and ACN were all several orders of magnitude below bulk solution conductivities, suggesting the low $Li^+$ conductivity in these solvents compared to the ionic conductivity of the bulk electrolyte solution was not specific to POATS-PPO-based membranes.[19] Other nonaqueous membrane conductivity studies have suggested that the ability of fixed charge groups to dissociate in the nonaqueous solvent may be the rate-limiting step for ionic conduction. In these studies, the use of $Li^+$ complexing agents in solution improved charge group dissociation and membrane conductivity increased up to 2 orders of magnitude above membranes soaked in solutions without additives.[46] Altogether, these results imply that the ion dissociation in the polymer phase is low and may be limiting the conductivity of the membrane. Although the measured IEC of these crosslinked membranes was high (2.5 mequiv $g^{-1}$), a low degree of dissociation would result in a low concentration of mobile charges in the membranes and could lead to the observed low fractions of solution conductivity in Figure 2b.

**Dissolved Active Material Permeability.** RFB membranes need to resist active material crossover to prevent capacity fade as the battery cycles. Ferrocene and 4-hydroxy-TEMPO were used as representative active materials because they have been used in nonaqueous RFBs, and in our previous work, these compounds had different thermodynamic interactions with the backbone polymer and different permeability through POATS-PPO membranes.[34] Permeability properties describe the tendency of the membrane to permit or block active material crossover. Ferrocene and 4-hydroxy-TEMPO permeability properties for the crosslinked membranes are reported in Figure 3.

In general, ferrocene permeability was greater than that of 4-hydroxy-TEMPO, which was consistent with previous reports,[34] but the use of different de-swelling solvents (and the resulting differences in solvent uptake) appeared to affect the magnitude of this difference. For example, the ratios of ferrocene permeability to 4-hydroxy-TEMPO permeability for high swelling membranes (i.e., membranes made using ethanol as the de-swelling solvent) were 2.0, 1.8, and 3.4 for PC, DMC, and ACN measurement solvents, respectively. In membranes that swell to a lesser extent (i.e., membranes made using ACN as the de-swelling solvent), the ratios increased in all cases, but

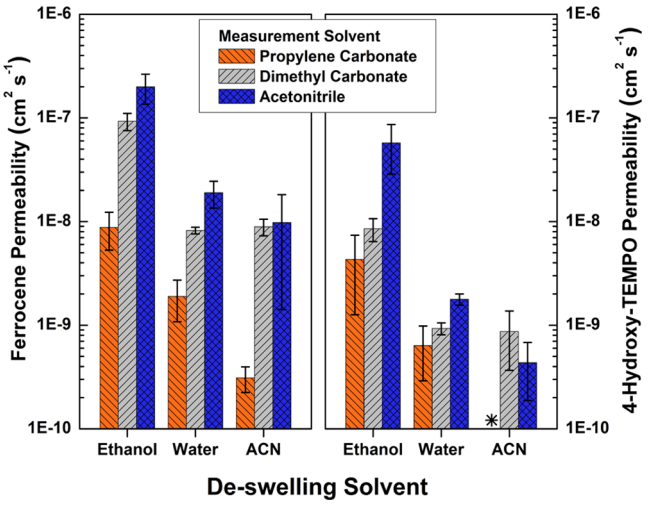


**Figure 3.** Ferrocene (left) and 4-hydroxy-TEMPO (right) permeability of crosslinked membranes made with different de-swelling solvents, immersed in measurement solvents: propylene carbonate (orange), dimethyl carbonate (gray), and acetonitrile (blue). The permeability of 4-hydroxy-TEMPO in the ACN/PC membrane, represented by *on the plot, was below the detection limit of $10^{-11}$ $cm^2$ $s^{-1}$. All reported values are the average of the values measured using three different membrane samples, and the reported uncertainty is the standard deviation of each membrane set.

to different extents: ≥31.1, 6.5, and 22.6 for PC, DMC, and ACN measurement solvents, respectively. This difference in selectivity was consistent with a general trade-off relationship between permeability and selectivity that has been previously observed in other systems, where more permeable membranes tend to be less selective.[24,26,55] In this case, the change in selectivity was different for each measurement solvent, but this may be because the change in solvent uptake from ACN de-swelled membranes to the ethanol de-swelled membranes was also different for each measurement solvent.

In general, higher uptake of a given measurement solvent resulted in higher permeability for both active materials. This trend was expected as permeability often correlates strongly with solvent uptake.[20,44] However, this general relationship would also lead one to expect that permeability values would be highest when PC was used as the measurement solvent since the PC measurement solvent led to higher solvent uptake compared to DMC or ACN (Figure 1a). Comparison of Figures 1a and 3 revealed that the opposite was true. Ferrocene and 4-hydroxy-TEMPO permeability values were lower when PC was used as the measurement solvent compared to the cases where either ACN or DMC measurement solvents were used even though solvent uptake was greatest when PC was used as the measurement solvent.

This unexpected result may be additional evidence that the higher solvent volume fraction observed with the PC measurement solvent was due to the preferential solvation of the charged regions of the polymer. Our previous study found that uncharged active material permeation may occur primarily in the uncharged, PPO backbone-rich, regions of POATS-PPO.[34] Additionally, changing the IEC of the membrane had a negligible influence on uncharged molecule permeability despite changes in solvent uptake.[23] Together, these results suggested that solvent uptake which occurs preferentially in the charged regions of the polymer may have a smaller effect on uncharged molecule permeability properties compared to


https://doi.org/10.1021/acsapm.2c02121
ACS Appl. Polym. Mater. 2023, 5, 2449−2461

changes in the solvent uptake of the uncharged regions of the polymer. The conductivity as a fraction of solution conductivity was also higher when PC (as opposed to DMC or ACN) was the measurement solvent (Figure 2b), and this observation could also be explained by preferential PC solvation of the charged regions of POATS-PPO compared to the other measurement solvents.

The permeability property differences between the three measurement solvents may be investigated in more detail using a free volume-based description of transport. In an extension of the model originally developed by Yasuda et al. (based on the work of Cohen and Turnbull),[56,57] the permeability, $P$, can be related to the volume fraction of solvent in the polymer, $\Phi$, as

$$P = P_0 \exp\left[-\frac{B}{\Phi}\right] \quad (7)$$

where $P_0$ and $B$ are taken as constants.[58] These constants are related to several factors, where $P_0$ is a constant related to the solution diffusivity and sorption coefficient, and $B$ is related to the proportionality constant between membrane solvent uptake and free volume available for transport and the permeant size, or, more specifically, the minimum free volume element size required for the permeating molecule to execute a diffusion step.[44] Therefore, permeability data correlated with $1/\Phi$ can provide insight into membrane structural factors that may be sensitive to the use of different measurement solvents.

The relationship between permeability and solvent volume fraction is shown as permeability vs the inverse of the solvent volume fraction in Figure 4. At an inverse solvent volume fraction of 1, the trend line should pass through the point equivalent to the diffusion coefficient of the molecule in bulk solution (Table 1), on the vertical axis. This requirement was because the product of the diffusion coefficient of the molecule in bulk solution and the partition coefficient for bulk solution (equal to unity) was the effective permeability of the bulk solution, which corresponded to $\Phi = 1$.[44] In Figure 4, the trend lines were constrained to pass through the diffusion coefficient of the molecule in bulk solution (Table 1) when $\Phi = 1$, and the slope was determined via linear regression.

The intercept of the trend line for the PC measurement solvent at $\Phi = 1$ was lower than the intercepts for the DMC or ACN measurement solvent trend lines in a manner consistent with the diffusion coefficients of the molecules in bulk solution (Table 1). These differences stemmed from differences in solution viscosity; PC had a significantly higher viscosity than DMC or ACN (2.52 vs 0.59 cP and 0.34 cP, respectively, Table 1) meaning that diffusion in PC was slower compared to DMC or ACN. Additionally, although ferrocene had a slightly higher molecular weight than 4-hydroxy-TEMPO (186 vs 172 g mol$^{-1}$), the ferrocene molar volume was slightly smaller (123 vs 145 mL mol$^{-1}$) than that of 4-hydroxy-TEMPO (calculations discussed in the Supporting Information). As a result, ferrocene diffusion coefficients in bulk solution were slightly greater compared to the situation for 4-hydroxy-TEMPO.

When ACN and DMC measurement solvents were used, permeability properties and the slopes of the best fit lines for both were similar for both ferrocene and 4-hydroxy-TEMPO. This result suggested that the solvated sizes of ferrocene and 4-hydroxy-TEMPO may be similar in the ACN or DMC solvents. Additionally, it suggested that the ACN and DMC solvents interacted with and impacted the polymer network similarly. This result was unexpected given the differences between ACN and DMC. ACN and DMC have different molecular weight and dielectric constant properties that might lead to differences in the size of the solvation shell of ferrocene or 4-hydroxy-TEMPO, and therefore differences in the minimum free volume element size required for diffusion (i.e., the slope of the trend lines in Figure 4).

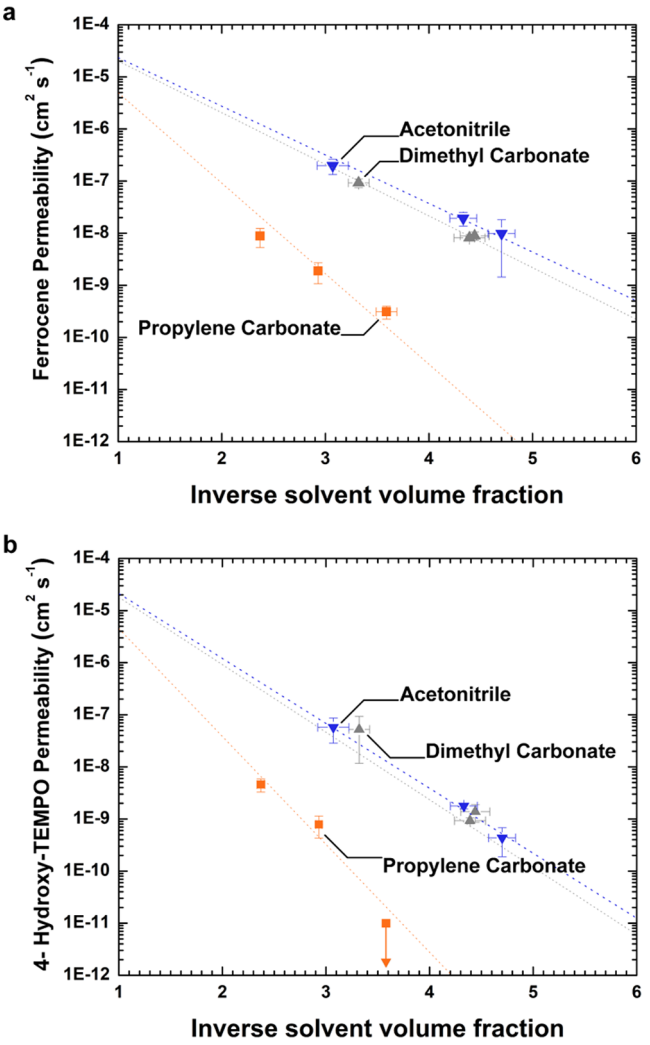


**Figure 4.** Permeability of (a) ferrocene and (b) 4-hydroxy-TEMPO reported as a function of inverse solvent volume fraction for electrolytes prepared using different measurement solvents: propylene carbonate (orange), dimethyl carbonate (gray), and acetonitrile (blue). Best fit lines are fixed to the diffusion coefficients of the molecules in bulk solution at inverse solvent volume fraction equal to 1. The permeability of 4-hydroxy-TEMPO in the ACN/PC membrane was below the detection limit and is reported as an upper bound of $10^{-11}$ cm$^2$ s$^{-1}$. All reported values are the average of the values measured using three different membrane samples, and the reported uncertainty is the standard deviation of each membrane set.

While the trend line slopes for both ferrocene and 4-hydroxy-TEMPO were similar when ACN and DMC were used as a measurement solvent, the trend lines when PC was used as the measurement solvent were steeper than ACN and DMC in both cases. To some extent, the lower permeability values may result from bulk solution properties (i.e., the diffusivity of ferrocene and 4-hydroxy-TEMPO in PC was slower than that in ACN or DMC). However, the steeper slope of the trend line for the PC measurement solvent data compared to that for the ACN or DMC measurement solvents



https://doi.org/10.1021/acsapm.2c02121
ACS Appl. Polym. Mater. 2023, 5, 2449−2461

Table 2. Tabulated Data for the Crosslinked POATS-PPO along with Nafion Data That Is Provided for Comparison

| membrane | de-swelling Solvent | measurement solvent | solvent uptake (%) | lithium-ion conductivity (mS $cm^{-1}$) | ferrocene permeability ($cm^2$ $s^{-1}$) | 4-hydroxy-TEMPO permeability ($cm^2$ $s^{-1}$) |
|---|---|---|---|---|---|---|
| crosslinked POATS-PPO | ethanol | propylene carbonate | 63.5 | 0.23 | $8.8 \times 10^{-9}$ | $4.6 \times 10^{-9}$ |
| | water | propylene carbonate | 45.3 | 0.20 | $1.9 \times 10^{-9}$ | $7.8 \times 10^{-10}$ |
| | acetonitrile | propylene carbonate | 33.7 | 0.20 | $3.1 \times 10^{-10}$ | $<1.0 \times 10^{-11}$ |
| | ethanol | dimethyl carbonate | 33.2 | 0.13 | $9.3 \times 10^{-8}$ | $5.2 \times 10^{-8}$ |
| | water | dimethyl carbonate | 22.8 | 0.15 | $8.2 \times 10^{-9}$ | $9.3 \times 10^{-10}$ |
| | acetonitrile | dimethyl carbonate | 22.4 | 0.14 | $8.9 \times 10^{-9}$ | $1.4 \times 10^{-9}$ |
| | ethanol | acetonitrile | 27.6 | 0.42 | $2.0 \times 10^{-7}$ | $5.8 \times 10^{-8}$ |
| | water | acetonitrile | 17.2 | 0.18 | $1.9 \times 10^{-8}$ | $1.8 \times 10^{-9}$ |
| | acetonitrile | acetonitrile | 15.4 | 0.18 | $9.8 \times 10^{-9}$ | $4.4 \times 10^{-10}$ |
| Nafion 117 | | propylene carbonate | 65[19] | 0.02[19] | $3 \times 10^{-8}$[20] | |
| | | dimethyl carbonate | 23[19] | 0.008[23] | $<1 \times 10^{-11}$[23] | |
| | | acetonitrile | 19[19] | 0.005[19] | $9.6 \times 10^{-9}$[59] | |

suggested that larger free volume elements were needed for ferrocene and 4-hydroxy-TEMPO to execute diffusional jumps in the membrane when PC was used as opposed to ACN or DMC, which could be the result of differences in solvation of either the active materials and/or the polymer.

Combining the permeability and conductivity results, these membranes had more favorable combinations of transport properties than Nafion in the same solvents. Comparisons of the data presented here to literature reports of Nafion are shown in Table 2. Overall, compared to the crosslinked POATS-PPO membranes, Nafion has low conductivity for lithium ions in the solvents used in this study. When measured in PC, the ACN de-swelled crosslinked membrane showed improved properties over Nafion, achieving both an order of magnitude higher conductivity and two orders of magnitude lower ferrocene permeability. The crosslinked membranes also had significantly higher conductivity than Nafion 117 in DMC and ACN, but the ferrocene permeability in ACN was similar for the crosslinked membranes and Nafion. In DMC, Nafion had much lower ferrocene permeability than the crosslinked membranes. Notably, there were crosslinked membranes with comparable solvent uptake to Nafion for all three measurement solvents, but in all solvents, the Nafion appeared to have more restricted transport, i.e., lower conductivity and similar or lower permeability at the same solvent uptake

Finally, although these crosslinked membranes have a much different synthesis procedure and composition than previously reported versions of POATS-PPO membranes, they continue to follow many trends that were noted in previous work. Ferrocene permeability continued to be independent of IEC for these crosslinked membranes, and the relation between IEC and the log of conductivity remains linear for the crosslinked membranes.[23] These trends and other comparisons to previous versions of the membrane materials are discussed in further detail in the Supporting Information.

## CONCLUSIONS

A crosslinking method for a sulfonated, PPO-based polymer was developed using an uncharged crosslinker and post-crosslinking solvent exchange steps to vary solvent uptake without significantly changing the membrane composition. The combination of crosslinking and solvent exchange steps revealed membrane properties that depended on both the specific de-swelling solvent used to prepare the membrane, which impacted solvent uptake, and the measurement solvent used to characterize the material.

Ionic conductivity was highest when ACN was used to characterize the membranes (up to 0.42 mS $cm^{-1}$), and this result was likely due to the significantly higher bulk solution conductivity of LiFSI in ACN compared to that in PC or DMC. The ionic conductivity and active material permeability were affected by both the de-swelling and measurement solvents, although with different trends for each solvent. Interestingly, free volume analysis suggested that the effective free volume element size required for transport was greater when PC was used as the measurement solvent compared to that for DMC and ACN. This observation suggested differences in the way that PC solvates the active materials and/or the polymer.

In this system, due to the differing dependence of conductivity and permeability on solvent uptake, membranes measured in PC had the most favorable combination of conductivity (0.20 mS $cm^{-1}$) and permeability (4-hydroxy-TEMPO, $<10^{-11}$ $cm^2$ $s^{-1}$). However, considering different redox shuttles, or the other impacts of using PC as the electrolyte solvent on the battery, could result in another solvent having the best overall performance in an RFB system. Also, since these effects appear to be a result of the specific interactions of PC with the membrane, these favorable material properties may be sensitive to the specific chemical composition of the polymer.

The solvent-specific effects reported in this work could be leveraged to prepare more effective membranes. Compared to prior versions of POATS-PPO, the membranes reported here achieved a higher fixed charge density (i.e., IEC) with more favorable mechanical properties and a combination of conductivity and permeability properties that was more desirable for RFB applications. The trends and observations reported here suggest that solvent-specific behavior will be critical for engineering membrane separators for nonaqueous redox flow battery applications.



https://doi.org/10.1021/acsapm.2c02121
ACS Appl. Polym. Mater. 2023, 5, 2449−2461

## ■ ASSOCIATED CONTENT

### Supporting Information

The Supporting Information is available free of charge at https://pubs.acs.org/doi/10.1021/acsapm.2c02121.

Additional experimental details including photographs of the membranes in several stages through the process, photographs of non-crosslinked membranes, $^1$H NMR spectra of the Br-PPO used in this work, a representative EIS spectrum used to measure ionic conductivity, additional experimental details of the UV/vis spectroscopy method used to measure concentrations, diffusion coefficient estimations, investigation of the possibility of membrane degradation or side reactions, discussion of area specific resistance and fixed charge concentrations, and comparisons of the membranes reported in this study to Nafion, as well as properties reported for similar preparations of these membrane materials (PDF)

## ■ AUTHOR INFORMATION


### Corresponding Authors

**Geoffrey M. Geise** − *Department of Chemical Engineering, University of Virginia, Charlottesville, Virginia 22903, United States;* orcid.org/0000-0002-5439-272X; Phone: +1 (434) 924-6248; Email: geise@virginia.edu

**Gary M. Koenig, Jr.** − *Department of Chemical Engineering, University of Virginia, Charlottesville, Virginia 22903, United States*; Phone: +1 (434) 982-2714; Email: gary.koenig@virginia.edu

### Author

**Patrick M. McCormack** − *Department of Chemical Engineering, University of Virginia, Charlottesville, Virginia 22903, United States*

Complete contact information is available at: https://pubs.acs.org/10.1021/acsapm.2c02121


### Notes

This report was prepared as an account of work sponsored by an agency of the United States Government. Neither the United States Government nor any agency thereof, nor any of their employees, makes any warranty, express or implied, or assumes any legal liability or responsibility for the accuracy, completeness, or usefulness of any information, apparatus, product, or process disclosed, or represents that its use would not infringe privately owned rights. Reference herein to any specific commercial product, process, or service by trade name, trademark, manufacturer, or otherwise does not necessarily constitute or imply its endorsement, recommendation, or favoring by the United States Government or any agency thereof. The views and opinions of authors expressed herein do not necessarily state or reflect those of the United States Government or any agency thereof.

The authors declare no competing financial interest.

## ■ ACKNOWLEDGMENTS

This research was funded by the National Science Foundation, through award IIP-1940915 and by the Department of Energy, Office of Nuclear Energy under Award Number DE-SC0022477.

## ■ REFERENCES


(1) Yousif, M.; Ai, Q.; Wattoo, W. A.; Jiang, Z.; Hao, R.; Gao, Y. Least Cost Combinations of Solar Power, Wind Power, and Energy Storage System for Powering Large-Scale Grid. *J. Power Sources* **2019**, *412*, 710−716.

(2) Johlas, H.; Witherby, S.; Doyle, J. R. Storage Requirements for High Grid Penetration of Wind and Solar Power for the MISO Region of North America: A Case Study. *Renewable Energy* **2020**, *146*, 1315−1324.

(3) Ziegler, M. S.; Mueller, J. M.; Pereira, G. D.; Song, J.; Ferrara, M.; Chiang, Y. M.; Trancik, J. E. Storage Requirements and Costs of Shaping Renewable Energy Toward Grid Decarbonization. *Joule* **2019**, *3*, 2134−2153.

(4) Darling, R. M.; Gallagher, K. G.; Kowalski, J. A.; Ha, S.; Brushett, F. R. Pathways to Low-Cost Electrochemical Energy Storage: A Comparison of Aqueous and Nonaqueous Flow Batteries. *Energy Environ. Sci.* **2014**, *7*, 3459−3477.

(5) Luo, J.; Hu, B.; Hu, M.; Zhao, Y.; Liu, T. L. Status and Prospects of Organic Redox Flow Batteries toward Sustainable Energy Storage. *ACS Energy Lett.* **2019**, *4*, 2220−2240.

(6) Ha, S.; Gallagher, K. G. Estimating the System Price of Redox Flow Batteries for Grid Storage. *J. Power Sources* **2015**, *296*, 122−132.

(7) Yuan, J.; Pan, Z.; Jin, Y.; Qiu, Q.; Zhang, C.; Zhao, Y.; Li, Y. Membranes in Non-Aqueous Redox Flow Battery: A Review. *J. Power Sources* **2021**, *500*, No. 229983.

(8) Wei, X.; Pan, W.; Duan, W.; Hollas, A.; Yang, Z.; Li, B.; Nie, Z.; Liu, J.; Reed, D.; Wang, W.; Sprenkle, V. Materials and Systems for Organic Redox Flow Batteries: Status and Challenges. *ACS Energy Lett.* **2017**, *2*, 2187−2204.

(9) Jia, C.; Pan, F.; Zhu, Y. G.; Huang, Q.; Lu, L.; Wang, Q. High − Energy Density Nonaqueous All Redox Flow Lithium Battery Enabled with a Polymeric Membrane. *Sci. Adv.* **2015**, *1*, No. e1500886.

(10) Zhou, M.; Huang, Q.; Pham Truong, T. N.; Ghilane, J.; Zhu, Y. G.; Jia, C.; Yan, R.; Fan, L.; Randriamahazaka, H.; Wang, Q. Nernstian-Potential-Driven Redox-Targeting Reactions of Battery Materials. *Chem* **2017**, *3*, 1036−1049.

(11) Zhu, Y. G.; Du, Y.; Jia, C.; Zhou, M.; Fan, L.; Wang, X.; Wang, Q. Unleashing the Power and Energy of LiFePO4-Based Redox Flow Lithium Battery with a Bifunctional Redox Mediator. *J. Am. Chem. Soc.* **2017**, *139*, 6286−6289.

(12) Gupta, D.; Zhang, Y.; Nie, Z.; Wang, J.; Koenig, G. M., Jr. Chemical Redox of Lithium-Ion Solid Electroactive Material in a Packed Bed Flow Reactor. *Chem. Eng. Sci.* **2022**, *251*, No. 117443.

(13) Zhang, F.; Gao, M.; Huang, S.; Zhang, H.; Wang, X.; Liu, L.; Han, M.; Wang, Q. Redox Targeting of Energy Materials for Energy Storage and Conversion. *Adv. Mater.* **2022**, *34*, No. 2104562.

(14) Ye, J.; Xia, L.; Wu, C.; Ding, M.; Jia, C.; Wang, Q. Redox Targeting-Based Flow Batteries. *J. Phys. D: Appl. Phys.* **2019**, *52*, No. 443001.

(15) Lehmann, M. L.; Tyler, L.; Self, E. C.; Yang, G.; Nanda, J.; Saito, T. Membrane Design for Non-Aqueous Redox Flow Batteries: Current Status and Path Forward. *Chem* **2022**, *8*, 1611−1636.

(16) Machado, C. A.; Brown, G. O.; Yang, R.; Hopkins, T. E.; Pribyl, J. G.; Epps, T. H. Redox Flow Battery Membranes: Improving Battery Performance by Leveraging Structure−Property Relationships. *ACS Energy Lett.* **2021**, *6*, 158−176.

(17) Xiong, P.; Zhang, L.; Chen, Y.; Peng, S.; Yu, G. A Chemistry and Microstructure Perspective on Ion-Conducting Membranes for Redox Flow Batteries. *Angew. Chem., Int. Ed.* **2021**, *60*, 24770−24798.

(18) Shi, Y.; Eze, C.; Xiong, B.; He, W.; Zhang, H.; Lim, T. M.; Ukil, A.; Zhao, J. Recent Development of Membrane for Vanadium Redox Flow Battery Applications: A Review. *Appl. Energy* **2019**, *238*, 202−224.

(19) Doyle, M.; Lewittes, M. E.; Roelofs, M. G.; Perusich, S. A.; Lowrey, R. E. Relationship between Ionic Conductivity of Perfluorinated Ionomeric Membranes and Nonaqueous Solvent Properties. *J. Membr. Sci.* **2001**, *184*, 257−273.

(20) Su, L.; Darling, R. M.; Gallagher, K. G.; Xie, W.; Thelen, J. L.; Badel, A. F.; Barton, J. L.; Cheng, K. J.; Balsara, N. P.; Moore, J. S.;

Brushett, F. R. An Investigation of the Ionic Conductivity and Species Crossover of Lithiated Nafion 117 in Nonaqueous Electrolytes. *J. Electrochem. Soc.* **2016**, *163*, A5253−A5262.
(21) Escalante-García, I. L.; Wainright, J. S.; Thompson, L. T.; Savinell, R. F. Performance of a Non-Aqueous Vanadium Acetylacetonate Prototype Redox Flow Battery: Examination of Separators and Capacity Decay. *J. Electrochem. Soc.* **2015**, *162*, A363−A372.
(22) Hudak, N. S.; Small, L. J.; Pratt, H. D.; Anderson, T. M. Through-Plane Conductivities of Membranes for Nonaqueous Redox Flow Batteries. *J. Electrochem. Soc.* **2015**, *162*, A2188−A2194.
(23) McCormack, P. M.; Luo, H.; Geise, G. M.; Koenig, G. M. Conductivity, Permeability, and Stability Properties of Chemically Tailored Poly(Phenylene Oxide) Membranes for Li+ Conductive Non-Aqueous Redox Flow Battery Separators. *J. Power Sources* **2020**, *460*, No. 228107.
(24) Geise, G. M.; Park, H. B.; Sagle, A. C.; Freeman, B. D.; McGrath, J. E. Water Permeability and Water/Salt Selectivity Tradeoff in Polymers for Desalination. *J. Membr. Sci.* **2011**, *369*, 130−138.
(25) Robeson, L. M.; Hwu, H. H.; McGrath, J. E. Upper Bound Relationship for Proton Exchange Membranes: Empirical Relationship and Relevance of Phase Separated Blends. *J. Membr. Sci.* **2007**, *302*, 70−77.
(26) Zhang, H.; Geise, G. M. Modeling the Water Permeability and Water/Salt Selectivity Tradeoff in Polymer Membranes. *J. Membr. Sci.* **2016**, *520*, 790−800.
(27) Geise, G. M.; Hickner, M. A.; Logan, B. E. Ionic Resistance and Permselectivity Tradeoffs in Anion Exchange Membranes. *ACS Appl. Mater. Interfaces* **2013**, *5*, 10294−10301.
(28) Li, Y.; Sniekers, J.; Malaquias, J. C.; Van Goethem, C.; Binnemans, K.; Fransaer, J.; Vankelecom, I. F. J. Crosslinked Anion Exchange Membranes Prepared from Poly(Phenylene Oxide) (PPO) for Non-Aqueous Redox Flow Batteries. *J. Power Sources* **2018**, *378*, 338−344.
(29) Small, L. J.; Pratt, H. D.; Fujimoto, C. H.; Anderson, T. M. Diels Alder Polyphenylene Anion Exchange Membrane for Non-aqueous Redox Flow Batteries. *J. Electrochem. Soc.* **2016**, *163*, A5106−A5111.
(30) Kwon, H.-G.; Bae, I.; Choi, S.-H. Crosslinked Poly(Arylene Ether Ketone) Membrane with High Anion Conductivity and Selectivity for Non-Aqueous Redox Flow Batteries. *J. Membr. Sci.* **2021**, *620*, No. 118928.
(31) Maurya, S.; Shin, S. H.; Sung, K. W.; Moon, S. H. Anion Exchange Membrane Prepared from Simultaneous Polymerization and Quaternization of 4-Vinyl Pyridine for Non-Aqueous Vanadium Redox Flow Battery Applications. *J. Power Sources* **2014**, *255*, 325−334.
(32) Paul, M.; Park, H. B.; Freeman, B. D.; Roy, A.; McGrath, J. E.; Riffle, J. S. Synthesis and Crosslinking of Partially Disulfonated Poly(Arylene Ether Sulfone) Random Copolymers as Candidates for Chlorine Resistant Reverse Osmosis Membranes. *Polymer* **2008**, *49*, 2243−2252.
(33) Park, J.-S.; Park, S.-H.; Yim, S.-D.; Yoon, Y.-G.; Lee, W.-Y.; Kim, C.-S. Performance of Solid Alkaline Fuel Cells Employing Anion-Exchange Membranes. *J. Power Sources* **2008**, *178*, 620−626.
(34) McCormack, P. M.; Koenig, G. M.; Geise, G. M. Thermodynamic Interactions as a Descriptor of Cross-Over in Nonaqueous Redox Flow Battery Membranes. *ACS Appl. Mater. Interfaces* **2021**, *13*, 49331−49339.
(35) Guillen, G. R.; Pan, Y.; Li, M.; Hoek, E. M. V. Preparation and Characterization of Membranes Formed by Nonsolvent Induced Phase Separation: A Review. *Ind. Eng. Chem. Res.* **2011**, *50*, 3798−3817.
(36) Mulder, M. *Basic Principles of Membrane Technology*, 2nd ed.; Springer: Netherlands, 1996.
(37) Jauhiainen, T. -P. Effect of Bromine and Phosphorus Substituents on the Glass Transition Properties of Some Substituted Poly(Oxy-1,4-phenylenes). *Angew. Makromol. Chem.* **1982**, *104*, 117−127.
(38) Li, N.; Yan, T.; Li, Z.; Thurn-Albrecht, T.; Binder, W. H. Comb-Shaped Polymers to Enhance Hydroxide Transport in Anion Exchange Membranes. *Energy Environ. Sci.* **2012**, *5*, 7888−7892.
(39) Chang, K.; Xue, T.; Geise, G. M. Increasing Salt Size Selectivity in Low Water Content Polymers via Polymer Backbone Dynamics. *J. Membr. Sci.* **2018**, *552*, 43−50.
(40) Han, H. B.; Zhou, S. S.; Zhang, D. J.; Feng, S. W.; Li, L. F.; Liu, K.; Feng, W. F.; Nie, J.; Li, H.; Huang, X. J.; Armand, M.; Zhou, Z. Bin. Lithium Bis(Fluorosulfonyl)Imide (LiFSI) as Conducting Salt for Nonaqueous Liquid Electrolytes for Lithium-Ion Batteries: Physicochemical and Electrochemical Properties. *J. Power Sources* **2011**, *196*, 3623−3632.
(41) Gong, K.; Fang, Q.; Gu, S.; Li, S. F. Y.; Yan, Y. Nonaqueous Redox-Flow Batteries: Organic Solvents, Supporting Electrolytes, and Redox Pairs. *Energy Environ. Sci.* **2015**, *8*, 3515−3530.
(42) Ding, M. S.; Xu, K.; Zhang, S.; Jow, T. R. Liquid/Solid Phase Diagrams of Binary Carbonates for Lithium Batteries Part II. *J. Electrochem. Soc.* **2001**, *148*, A299−A304.
(43) Gagliardi, L. G.; Castells, C. B.; Ràfols, C.; Rosés, M.; Bosch, E. Static Dielectric Constants of Acetonitrile/Water Mixtures at Different Temperatures and Debye-Hückel A and A0B Parameters for Activity Coefficients. *J. Chem. Eng. Data* **2007**, *52*, 1103−1107.
(44) Geise, G. M.; Paul, D. R.; Freeman, B. D. Fundamental Water and Salt Transport Properties of Polymeric Materials. *Prog. Polym. Sci.* **2014**, *39*, 1−42.
(45) Erb, A. J.; Paul, D. R. Gas Sorption and Transport in Polysulfone. *J. Membr. Sci.* **1981**, *8*, 11−22.
(46) Doyle, M.; Lewittes, M. E.; Roelofs, M. G.; Perusich, S. A. Ionic Conductivity of Nonaqueous Solvent-Swollen Ionomer Membranes Based on Fluorosulfonate, Fluorocarboxylate, and Sulfonate Fixed Ion Groups. *J. Phys. Chem. B* **2001**, *105*, 9387−9394.
(47) Zhang, X.; Kuroda, D. G. An Ab Initio Molecular Dynamics Study of the Solvation Structure and Ultrafast Dynamics of Lithium Salts in Organic Carbonates: A Comparison between Linear and Cyclic Carbonates. *J. Chem. Phys.* **2019**, *150*, No. 184501.
(48) Han, S.-D.; Borodin, O.; Seo, D. M.; Zhou, Z.-B.; Henderson, W. A. Electrolyte Solvation and Ionic Association: V. Acetonitrile-Lithium Bis(Fluorosulfonyl)Imide (LiFSI) Mixtures. *J. Electrochem. Soc.* **2014**, *161*, A2042−A2053.
(49) Borodin, O.; Smith, G. D. Quantum Chemistry and Molecular Dynamics Simulation Study of Dimethyl Carbonate: Ethylene Carbonate Electrolytes Doped with LiPF6. *J. Phys. Chem. B* **2009**, *113*, 1763−1776.
(50) Kondou, S.; Sakashita, Y.; Yang, X.; Hashimoto, K.; Dokko, K.; Watanabe, M.; Ueno, K. Li-Ion Transport and Solvation of a Li Salt of Weakly Coordinating Polyanions in Ethylene Carbonate/Dimethyl Carbonate Mixtures. *ACS Appl. Mater. Interfaces* **2022**, *14*, 18324−18334.
(51) Chapman, N.; Borodin, O.; Yoon, T.; Nguyen, C. C.; Lucht, B. L. Spectroscopic and Density Functional Theory Characterization of Common Lithium Salt Solvates in Carbonate Electrolytes for Lithium Batteries. *J. Phys. Chem. C* **2017**, *121*, 2135−2148.
(52) Chang, K.; Geise, G. M. Dielectric Permittivity Properties of Hydrated Polymers: Measurement and Connection to Ion Transport Properties. *Ind. Eng. Chem. Res.* **2020**, *59*, 5205−5217.
(53) Matsumoto, K.; Endo, T. Synthesis of Networked Polymers by Copolymerization of Monoepoxy- Substituted Lithium Sulfonylimide and Diepoxy-Substituted Poly(Ethylene Glycol), and Their Properties. *J. Polym. Sci., Part A: Polym. Chem.* **2011**, *49*, 1874−1880.
(54) Lehmann, M. L.; Yang, G.; Nanda, J.; Saito, T. Unraveling Ion Transport in Trifluoromethanesulfonimide Pentablock Copolymer Membranes in Nonaqueous Electrolytes. *Macromolecules* **2022**, *55*, 7740−7751.
(55) Xie, W.; Ju, H.; Geise, G. M.; Freeman, B. D.; Mardel, J. I.; Hill, A. J.; McGrath, J. E. Effect of Free Volume on Water and Salt Transport Properties in Directly Copolymerized Disulfonated Poly-

(Arylene Ether Sulfone) Random Copolymers. *Macromolecules* **2011**, *44*, 4428−4438.
(56) Yasuda, H.; Lamaze, C. E.; Ikenberry, L. D. Permeability of Solutes through Hydrated Polymer Membranes. Part 1. Diffusion of Sodium Chloride. *Makromol. Chem.* **1968**, *118*, 19−35.
(57) Cohen, M. H.; Turnbull, D. Molecular Transport in Liquids and Glasses. *J. Chem. Phys.* **1959**, *31*, 1164−1169.
(58) Xie, W.; Geise, G. M.; Freeman, B. D.; Lee, C. H.; McGrath, J. E. Influence of Processing History on Water and Salt Transport Properties of Disulfonated Polysulfone Random Copolymers. *Polymer* **2012**, *53*, 1581−1592.
(59) Mushtaq, K.; Lagarteira, T.; Zaidi, A. A.; Mendes, A. In-Situ Crossover Diagnostics to Assess Membrane Efficacy for Non-Aqueous Redox Flow Battery. *J. Energy Storage* **2021**, *40*, No. 102713.





https://doi.org/10.1021/acsapm.2c02121
*ACS Appl. Polym. Mater.* 2023, 5, 2449−2461